UDC 544.18:544.723:546.26:546.72:546.17 doi: 10.15407/Surface.2023.15.003

STABILITY OF SINGLE-ATOM IRON COMPLEXES ON GRAPHENE DOUBLE VACANCY

O.S. Karpenko, V.V. Lobanov, M.T. Kartel

Chuiko Institute of Surface Chemistry of the NAS of Ukraine,
17 General Naumov Str., Kyiv 03164, Ukraine. E-mail: karpenkooksana@ukr.net

*The equilibrium and spatial structure of the polycyclic aromatic hydrocarbon $C_{96}H_{24}$, chosen as a model of the graphene plane, as well as the systems obtained from it by removing the diatomic molecule C_2 ($C_{94}H_{24}$) and then replacing four carbon atoms with four nitrogen atoms ($C_{90}N_4H_{24}$) have been studied by the DFT method (B3LYP) in the 6-31G** basis using Grimme corrections to account for dispersion interactions. In the same approximation, the energetics of the formation of a complex of an iron atom in zero oxidation degree (Fe^0) with $C_{90}N_4H_{24}$ ($[C_{90}N_4H_{24}Fe]^0$) in the square planar field of the ligand has been studied. The types of molecular orbitals of the ligand, which correspond to the symmetry of the atomic d-orbitals of the Fe atom, have been determined. Interaction diagrams of the d-orbitals of the Fe atom with some molecular orbitals of the ligand $C_{90}N_4H_{24}$ of the corresponding symmetry are constructed. It is concluded that the binding of the transition metal atom on the double vacancy of the graphene plane can be rationally described based on the local symmetry of the coordination center and molecular orbitals of the ligand and the formed complex.*

Keywords: *Fe-doped graphene, polycyclic aromatic hydrocarbon (PAH), density functional theory (DFT), defect-containing graphene, double vacancy, transition metal atom*, *ligand field theory.*

Immediately after the discovery of the possibility of obtaining a single layer of carbon atoms (graphene) [1], intensive research was started aimed at the practical use of its unique properties [2]. Graphene began to be used in various fields, from energy generation in hydrogen cells [3, 4] to the element base of microelectronics [5], in spintronic devices [6, 7] and sensor sensors [8, 9]. This versatility is at least partly due to its electronic structure, particularly the zero density of single electron states, at the Fermi energy level (Dirac point) [10]. This conclusion was first obtained in several theoretical works operating with graphene of ideal structure [11–14]. Experimental studies have shown that it is extremely difficult or even impossible to obtain graphene samples without various types of defects in its structure [15]. This raised the dilemma, of which is better – graphene of a highly perfect sample or – with controlled deviations from identity [11].

Since the uniqueness of ideal graphene is due to the zero density of states in the Dirac point, the introduction of various types of defects in its structure should be directed to the creation of a forbidden zone of single electron states, which gives it new functional properties.

The most effective methods of graphene functionalization consist of creating different types of vacancies in its crystal lattice [11] and replacing carbon atoms with heteroatoms, the

number of electrons that is less or more than that of the carbon atom, which leads to interesting effects and potential applications. No less fruitful can be the joint use of these approaches, opening the possibility of creating active centers of different natures, which provide binding of molecules or atoms, including transition metal (TM) atoms, which have high catalytic properties. Depending on the nature of the adsorption complex formed, it is possible to control the width of the resulting forbidden gap of graphene, bandgap, optical, metallic, and chemical (catalytic) properties [16–19].

To better explain the properties of adsorption complexes of defect-containing doped graphene with a single TM atom, it is advisable to involve the concepts of classical coordination chemistry, which will help to elucidate some aspects that are not manifested in the framework of a simple approach about the interaction between the adsorbent surface and the adsorbed atom [20, 21]. In this case, the graphene sample can be considered as a multifunctional ligand concerning the transition *d*-metal atom or ion. A similar situation is realized in chelate complexes or metal-containing porphyrin and phthalocyanine complexes.

The *d*-metal complexes are important in inorganic chemistry, materials science, and nanotechnology. The method used to describe the nature of the ligand-metal bond is based on crystal field theory, which uses a clear and simple electrostatic model [22]. The crystal field theory does not explain many physical properties of TM complexes because it does not take into account the interaction between the metal and ligand orbitals. In a more sophisticated approach based on molecular orbital theory, the ligand field theory, it is assumed that the metal atom is surrounded by ions or molecules from which electron density is transferred to the TM atom to form a metal-ligand bond [23]. The stability of the complexes is mainly determined by attraction interactions, but repulsion interactions lead to a secondary effect that accounts for 10% of the total energy but has significant implications for the trends observed in *d*-metal complexes.

Molecular orbital theory can be successfully applied to TM complexes to explain both the covalent and ionic nature of the bonding between the metal atom and the ligands.

A TM atom or ion has a set of nine valence atomic orbitals (AOs) that can participate in molecular orbitals (MOs) formation. It consists of five n*d*, three (n+1)*p* and one (n+1)*s* orbitals. For the iron atom, the principal quantum number is n=3 and the electronic configuration can be written as $1s^2 2s^2 2p^6 3s^2 3p^6 3d^6 4s^2$. Its *d*-AOs have energies corresponding to binding to ligands. The success of the application of molecular orbital theory is determined by the geometry of the complex and can be used to describe the properties of octahedral, tetrahedral, and square complexes. Complexes of iron atoms or their ions Fe^{2+}, and Fe^{3+}, which are formed by their binding by graphene-like planes containing vacancies, can be referred to them.

The peculiarities of the application of the molecular orbital theory for *d*-metal complexes are as follows:

1) the AO of the metal center and the group abundances of the surrounding ligands or multifunctional ligand (in the latter case, the MO of the ligand should be considered) unite to form the MO of the complex;

2) as a result of their additive overlap, bonding MOs are formed, and in subtractive overlap, anti-bonding molecular orbitals are formed;

3) the energy of the bonding MO is lower than the energies of the constituent AOs, while the energy of the antibonding ones is higher;

4) the ionic character of covalent bonding arises from the difference in the energy of the AOs involved in the formation of the MO of the complex;

5) if the energy of the MO of the complex is comparable to the energy of the AO of the metal atom, then such an MO will not differ significantly from the AO in nature and can be considered non-bonding.

The anchoring of a TM atom on graphene can be regarded as the formation of a coordination complex. The combined use of the concepts of solid state theory (Fermi level, zone

structure, bandgap, bandgap width) and concepts of classical coordination chemistry (central ion or atom, ligand, splitting in the field of ligands, types of symmetry of the crystal field) allows us to deepen the knowledge in the field of single-atom functionalization of graphene and to elucidate the factors affecting the properties of materials based on graphene.

In the proposed paper we present data obtained by the DFT method (B3LYP, 6-31G**) [24, 25] using the software module [26] with the involvement of Grimme corrections to account for dispersion interactions) [27, 28], regarding the energetics of the formation of a double vacancy in a carbon material, its decoration with nitrogen atoms, and the formation of a complex with one iron atom.

The polycyclic aromatic hydrocarbon (PAH) $C_{96}H_{24}$ of hexagonal structure, shown in Fig. 1 *a*, was chosen as a model of graphene. According to the results of the performed calculations, the formation of a diatomic vacancy (V_2-type defect), i.e., the removal of a two-atom C_2 molecule from the $C_{96}H_{24}$ molecule, is an endothermic process with a reaction energy (E_{react}) of 16.73 eV (see Fig. 1 *b*). The replacement of four carbon atoms by four nitrogen atoms in the $C_{94}H_{24}$ molecular system containing a double vacancy to form the new $C_{90}N_4H_{24}$ system is also an endothermic process with E_{react} = 7.77 eV (see Fig. 2). The ground electronic state (GES) of the molecular systems $C_{94}H_{24}$ and $C_{90}N_4H_{24}$ is singlet, i.e., their multiplicity (M) is equal to one. As a result, based on the PAH $C_{96}H_{24}$, a coordination node of symmetry D_{4h}, consisting of four nitrogen atoms, capable of binding a single iron atom containing four unpaired electrons on 3*d*-orbitals is formed. The energy of the complex formation $[C_{90}N_4H_{24}Fe]^0$ (M=3) (see Fig. 3) involving a neutral iron atom and nitrogen-containing ligand $C_{90}N_4H_{24}$ is -7.37 eV.

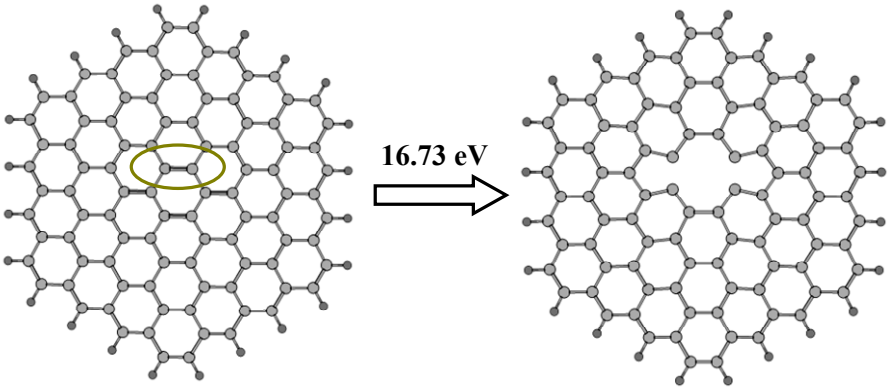

Fig. 1. Equilibrium structure of the molecule $C_{96}H_{24}$ and the system obtained by removing the diatomic molecule C_2 from it.

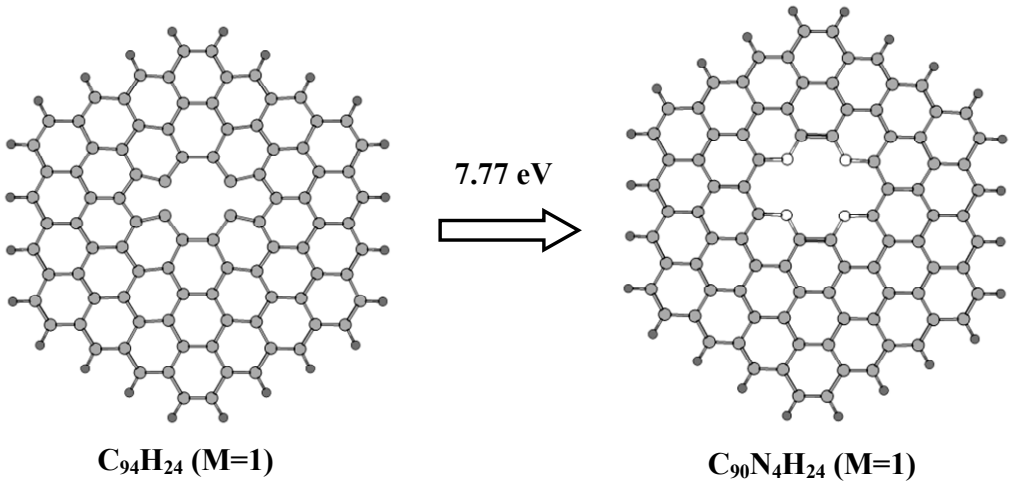

Fig. 2. Equilibrium structure of $C_{94}H_{24}$ and $C_{90}N_4H_{24}$ systems.

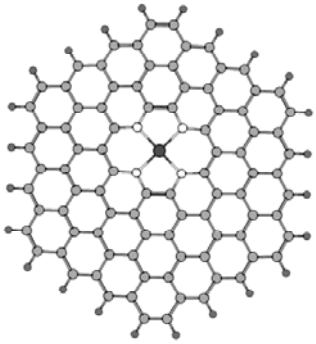

$[C_{90}N_4H_{24}Fe]^0$ (M=3)

Fig. 3. Equilibrium structure of the complex $[C_{90}N_4N_{24}Fe]^0$ (M=3).

In the equilibrium state of the defect-containing, nitrogen atom-decorated $C_{90}N_4H_{24}$ system, the N atoms are located at the vertices of a rectangle with sides 2.779 and 2.652 Å, which differs slightly from a square. The diagonal of this rectangle is 3.840 Å and, considering that the radii of Fe and N atoms are 1.26 and 0.71 Å, respectively [29], it can be argued that the size of the cavity under consideration favors the introduction of an iron atom into it and the planar structure of the $[C_{90}N_4N_{24}Fe]^0$ complex.

Classical coordination complexes can be used as a model to understand the chemical and spectroscopic properties of TM atoms coordinated on graphene functional groups. Macrocyclic ligands such as porphyrins and phthalocyanine have similar structures compared to sites where four C atoms on V_2 defects are replaced by four N atoms (N_4-graphene). The complexes of the "TM atom-N_4-graphene" type show a planar structure with local D_{4h} symmetry. In this case, the ligand-field splitting diagram of the *d*-orbitals level of the free atom will be similar to that of the square planar complex (Fig. 5). Where d_{xz} and d_{yz} are doubly degenerate orbitals of e_g symmetry; d_{z2} orbital has a_{1g} symmetry; d_{x2-y2} orbital has b_{1g} symmetry; d_{xy} orbital has b_{2g} symmetry. Due to the absence of ligands at the axial position of the complex, the d_{z2}-orbital of the TM atom with lobes on the *z*-axis has lower energy compared to the d_{xy} and d_{x2-y2} orbitals. Attention should be paid to the main difference between the splitting of the *d*-orbital level in the square planar complex and the splitting in the octahedral and tetrahedral ligand fields. In the latter two cases, the *d*-orbitals are split into two groups of closely spaced levels with a well-defined difference between the groups, precisely determining the splitting value $10D_g$, which is not possible for the planar field.

For the equilibrium spatial structure of the $[C_{90}N_4H_{24}Fe]^0$ complex, the diagonal of the rectangle formed by the four nitrogen atoms of the coordination site is 3.808 Å, which is 0.032 Å smaller than in the nitrogen atom-decorated ligand. Such a noticeable decrease in the N···N distance indicates the formation of the Fe–N coordination bond, the order of which is 0.474.

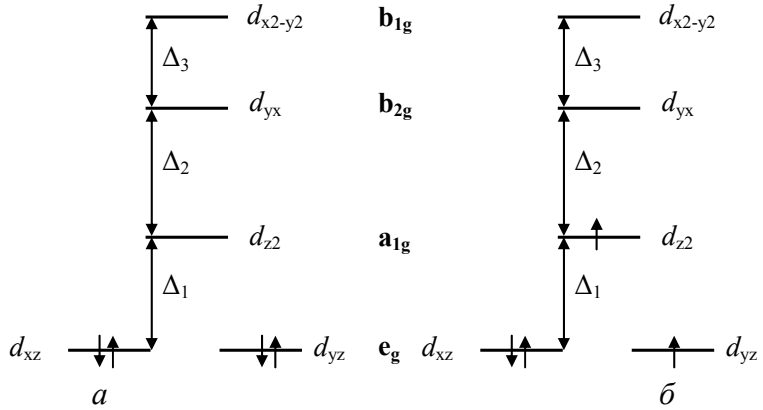

Fig. 5. Qualitative picture of the splitting of the five-fold-degenerate energy level of *d*-orbitals of the iron atom in a planar square field of ligands: (*a*) – singlet state; (*b*) – the lowest in energy triplet state.

Fig. 6 shows the structure of two frontal MOs of the ligand ($C_{90}N_4H_{24}$) HOMO-5 (*a*) and HOMO-4 (*b*), localized exclusively in the coordination center region and on which the σ-bonding electrons are concentrated. The other frontal MOs of the ligand have π-symmetry (see Fig. 7). Analyzing the MO structure of HOMO-5, HOMO-4, and LUMO π-orbitals of the ligand $C_{90}N_4H_{24}$, it can be stated that the formation of complexes with a single atom of the transition element is possible only due to σ-bonding with its *d*-orbitals. Binding with the formation of π-bonds are excluded due to the symmetry conditions. This is confirmed by the structure of the frontal MOs of the $[C_{90}N_4H_{24}Fe]^0$ complex.

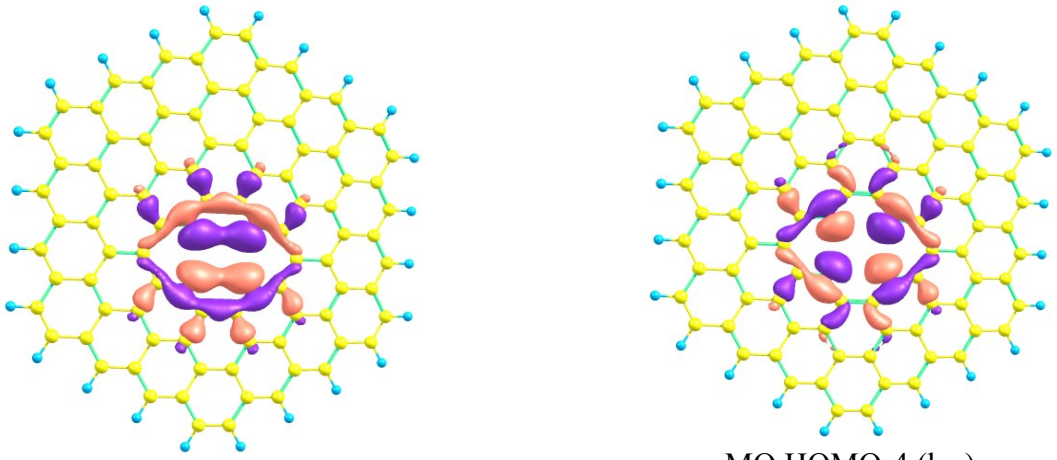

MO HOMO-5 (a_{1g}) MO HOMO-4 (b_{1g})

Fig. 6. Structure of two frontal MOs NOMO-5 and NOMO-4 localized in the vicinity of the coordination center of ligand $C_{90}N_4H_{24}$.

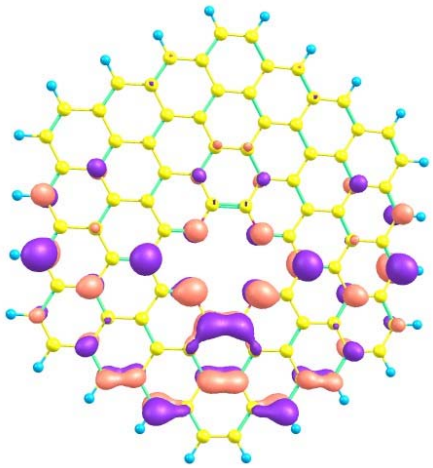

Fig. 7. Structure of the frontal LUMO π-orbital localized in the vicinity of the coordination center of the ligand $C_{90}N_4H_{24}$.

Fig. 8 shows the structure of the frontal MOs of the complex $[C_{90}N_4H_{24}Fe]^0$, formed by the binding of a single iron atom by the ligand $C_{90}N_4H_{24}$. Since the GES multiplicity of the $[C_{90}N_4H_{24}Fe]^0$ complex is three, both, α- and β-subsystems should be considered. Fig. 8 *a* shows that in the MO HOMO(α)-2, the predominant contribution is made by the AO d_{x2-y2} (b_{1g} symmetry) of the Fe atom and the σ-orbitals of the nitrogen atom bonding to the nearest carbon atoms. The MO HOMO(α)-4 is formed from the AO d_{z2} of the Fe atom, and an insignificant contribution from the orbitals of the four nitrogen atoms.

Direct calculations of the complex $[C_{90}N_4H_{24}Fe]^0$ in various spin states showed that, as already noted, the GES corresponds to the triplet, which is only 1.43 eV away from the singlet state. Thus, the electron distribution over single-electron levels in the $[C_{90}N_4N_{24}Fe]^0$ complexes is reproduced by Fig. 5 *b*, indicating that the field strength of the ligand is sufficient for the electron splitting from one of the doubly degenerate d_{xz} or d_{yz} orbitals.

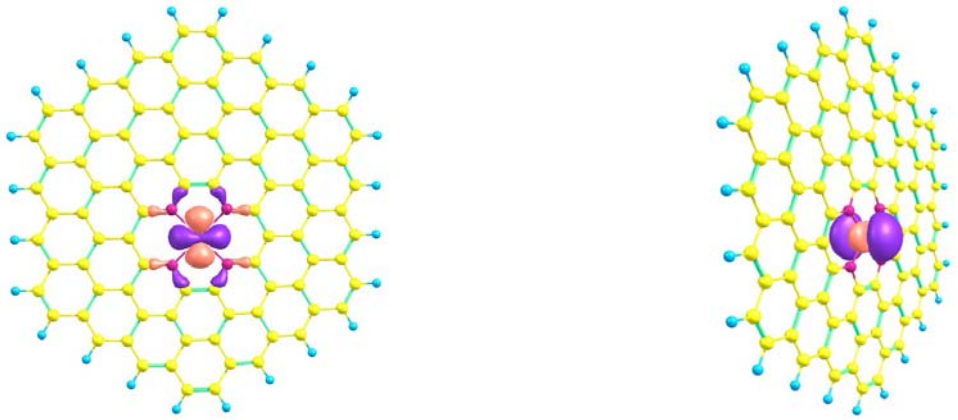

HOMO(α)-2 (a_{1g}) HOMO(α)-4 (b_{1g})

Fig. 8. Structure of two frontal MOs HOMO(α)-2 and HOMO(α)-4 localized in the vicinity of the coordination center of the $[C_{90}N_4H_{24}Fe]^0$ complex

Analysis of the MO energies of the ligand $C_{90}N_4H_{24}$ and the complex $[C_{90}N_4H_{24}Fe]^0$ showed that the orbital d_{x2-y2} of the iron atom interacts with the MO HOMO-5 (a_{1g}) (energy -5.92 eV) of the ligand to form two MOs – one bonding (energy -6.72 eV) and one antibonding (energy -5.53 eV) (see Fig. 9). A similar picture takes place regarding the interaction of the d_{z2} orbital of the iron atom with the MO HOMO-4 (b_{1g}) of the ligand $C_{90}N_4H_{24}$, which is shown in Fig. 10.

It is necessary to make a small remark concerning the choice of the energy level of the *d*-orbitals of the iron atom, the GES multiplicity of which is equal to 5. Formally, the iron atom has two electronic subsystems *α* and *β*, i.e., the energies of all 5*d*-orbitals should be somewhat different. Therefore, the HOAO energy of the *α*-subsystem was chosen for the orbital energy level, and the HOAO energy of the *β*-subsystem was chosen for the orbital energy level.

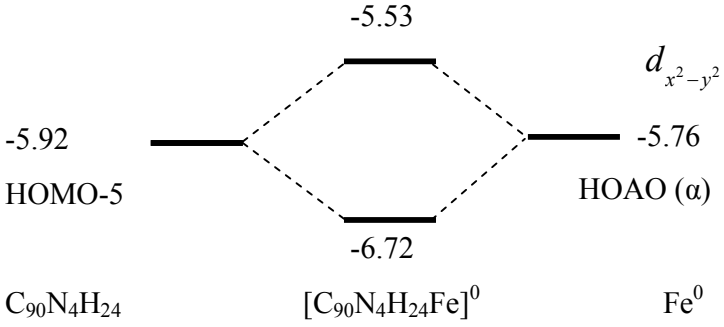

Fig. 9. MO energy levels of the $C_{90}N_4H_{24}$ ligand, the $[C_{90}N_4H_{24}Fe]^0$ complex, and the atomic orbital of the iron atom.

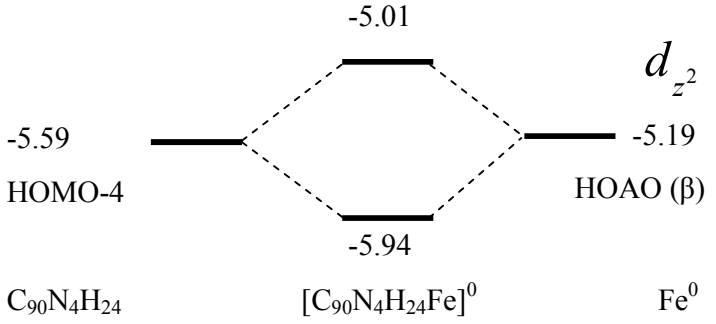

Fig. 10. MO energy levels of the $C_{90}N_4H_{24}$ ligand, the $[C_{90}N_4H_{24}Fe]^0$ complex, and the atomic orbital of the iron atom.

To summarize, we note:

– the binding of the TM atom on graphene can be rationalized based on the local symmetry of the coordination center and the MOs of the ligand and the formed complex;

– *d*-orbitals of the TM atom can be mixed with MOs of graphene of the same symmetry, which leads to redistribution of MOs by energy and, as a consequence, to the change of splitting in the ligand field;

– the formation of graphene-like complexes with one Fe atom is possible only due to σ-bonding. Binding with the formation of π-bonds is excluded due to symmetry conditions.

References

1. Novoselov K.S., Geim A.K., Morozov S.V., Jiang D., Zhang Y., Dubonos S.V., Grigorieva I.V., Firsov A.A. Electric field effect in atomically thin carbon films. *Science*. 2004. **306**(5696): 666. https://doi.org/10.1126/science.1102896
2. Castro Neto A.H., Guinea F., Peres N.M.R., Novoselov K.S., Geim A.K. The electronic properties of graphene. *Rev. Modern Phys*. 2009. **81**(1):109. https://doi.org/10.1103/RevModPhys.81.109
3. Geng, D. S., Chen Y., Chen Y.G. Li Y.L., Li R.Y., Sun X.L., Ye S.Y., Knights S. High oxygen-reduction activity and durability of nitrogen-doped graphene. *Energy Environ. Sci.* 2011. **4**: 760. https://doi.org/10.1039/C0EE00326C
4. Shao Y.Y., Zhang S., Engelhard M.H., Li G.S., Shao G.C., Wang Y., Liu J., Aksay I.A., Lin Y.H. Nitrogen-doped graphene and its electrochemical applications. *J. Mater. Chem*. 2010. **20**(35): 7491−7496. https://doi.org/10.1039/C0JM00782J
5. Javey A., Guo J., Farmer D.B., Wang Q., Wang D., Gordon R.G., Lundstrom M., Dai H. Carbon nanotube field-effect transistors with integrated ohmic contacts and high-κ gate dielectrics. *Nano Lett*. 2004. **4**(3): 447–450. https://doi.org/10.1021/nl035185x
6. Karpan V.M., Giovannetti G., Khomyakov P.A., Talanana M., Starikov A.A., Zwierzycki M., van den Brink J., Brocks G., Kelly P.J. Graphite and graphene as perfect spin filters. *Phys. Rev. Let*. 2007. **99**(17): 176602. https://doi.org/10.1103/PhysRevLett.99.176602
7. Tombros N., Jozsa C., Popinciuc M., Jonkman H.T., van Wees B.J. Electronic spin transport and spin precession in single graphene layers at room temperature. *Nature*. 2007. **448**(7153): 571–574. https://doi.org/10.1038/nature06037
8. Rumyantsev S., Liu G., Shur M.S., Potyrailo R.A., Balandin A.A. Selective gas sensing with a single pristine graphene transistor. *Nano Lett*. 2012. **12**(5): 2294–2298. https://doi.org/10.1021/nl3001293
9. Jebreiil Khadem S.M., Abdi Y., Darbari S., Ostovari F. Investigating the effect of gas absorption on the electromechanical and electrochemical behavior of graphene/ZnO structure, suitable for highly selective and sensitive gas sensors. *Curr. Appl. Phys*. 2014. **14**(11): 1498–1503. http://dx.doi.org/10.1016/j.cap.2014.07.020
10. Novoselov K.S., Geim A.K., Morozov S.V., Jiang D., Katsnelson M.I., Grigorieva I.V., Dubonos S.V., Firsov A.A. Two-dimensional gas of massless Dirac fermions in graphene. *Nature*. 2005. **438**: 197–200. https://doi.org/10.1038/nature04233
11. Banhart F., Kotakoski J., Krasheninnikov A.V. Structural defects in graphene. *ACS Nano.* 2011. **5**(1): 26–41. https://doi.org/10.1021/nn102598m
12. Krasheninnikov A.V., Lehtinen P.O., Foster A.S., Nieminen R.M. Bending the rules: contrasting vacancy energetics and migration in graphite and carbon nanotubes. *Chem. Phys. Lett*. 2006. **418**: 132–136. https://doi.org/10.1016/j.cplett.2005.10.106
13. Rossato J., Baierle R.J., Fazzio A., Mota R. Vacancy formation process in carbon nanotubes: first-principles approach. *Nano Lett*. 2005. **5**(1): 197–200. https://doi.org/10.1021/nl048226d

14. El-Barbary A.A., Telling R.H., Ewels C.P., Heggie M.I., Briddon P.R. Structure and energetics of the vacancy in graphite. *Phys. Rev. B*. 2003. **68**(14): 144107. https://doi.org/10.1103/PhysRevB.68.144107
15. Gerber I.C., Serp P. A theory/experience description of support effects in cabon-supported catalyst. *Chem. Rev*. 2020. **120**(2): 1250–1349. https://doi.org/10.1021/acs.chemrev.9b00209
16. Santos E.J.G., Ayuela A., Sánchez-Portal D. First-principles study of substitutional metal impurities in graphene: structural, electronic and magnetic properties. *New J. Phys*. 2010. **12**: 053012. https://doi.org/10.1088/1367-2630/12/5/053012
17. Hou C., Wang J., Du W., Wang J., Du Y., Liu C., Zhang J., Hou H., Dang F., Zhao L., Guo Z. One-pot synthesized molybdenum dioxide–molybdenum carbide heterostructures coupled with 3D holey carbon nanosheets for highly efficient and ultrastable cycling lithium-ion storage. *J. Mater. Chem. A*. 2019. **7**(22): 13460–13472. https://doi.org/10.1039/C9TA03551F
18. Kumar R., Kumar R.S., Pratap D.S., Joanni E., Manohar R.Y., Moshkalev S.A. Laser-assisted synthesis, reduction and micro-patterning of graphene: Recent progress and applications Author links open overlay panel. *Coord. Chem. Rev*. 2017. **342**: 34–79. https://doi.org/10.1016/j.ccr.2017.03.021
19. Le K., Wang Z., Wang F., Wang Q., Shao Q., Murugadoss V., Wu S., Liu W., Liu J., Gao Q., Guo Z. Sandwich-like NiCo layered double hydroxide/reduced graphene oxide nanocomposite cathodes for high energy density asymmetric supercapacitors. *Dalton Trans*. 2019. **48**(16): 5193–5202. https://doi.org/10.1039/C9DT00615J
20. Grasseschi D., Silva W.C., de Souza Paiva R., Starke L.D., do Nascimento A.S. Surface coordination chemistry of graphene: Understanding the coordination of single transition metal atoms. *Coord. Chemi. Rev*. 2020. **422**: 213469. https://doi.org/10.1016/j.ccr.2020.213469
21. Wood J.S. Ligand Field Theory. *Nature*. 1970. **226**: 1067–1068. https://doi.org/10.1038/2261067c0
22. Zuckerman J.J. Crystal field splitting diagrams. *J. Chem. Educ*. 1965. **42**(6): 315. https://doi.org/10.1021/ed042p315
23. Liehr A.D. A comparison of theories: Molecular orbital, valence bond, and ligand field. *J. Chem. Educ*. 1962. **39**(3): 135. https://doi.org/10.1021/ed039p135
24. Becke A.D. Density functional thermochemistry. III. The role of exact exchange. *J. Chem. Phys*. 1993. **98**(7): 5648–5652. https://doi.org/10.1063/1.464913
25. Lee C., Yang W., Parr R.G. Development of the Colle-Salvetti correlation-energy formula into a functional of the electron density. *Phys. Rev. B*. 1988. **37**(2): 785. https://doi.org/10.1103/PhysRevB.37.785
26. Schmidt M.W., Baldridge K.K., Boatz J.A., Elbert S.T., Gordon M.S., Jensen J.H., Koseki S., Matsunaga N., Nguyen K.A., Su S., Windus T.L., Dupuis M., Montgomery Jr J.A. General atomic and molecular electronic structure system. *J. Comput. Chem*. 1993. 14(11): 1347–1363. https://doi.org/10.1002/jcc.540141112
27. Grimme S., Ehrlich S., Goerigk L. Effect of the damping function in dispersion corrected density functional theory. *J. Comput Chem*. 2011. **32**(7): 1456–1465. https://doi.org/10.1002/jcc.21759
28. Grimme S. Density functional theory with London dispersion corrections. *WIREs Comput. Mol. Sci*. 2011. **1**(2): 211–228. https://doi.org/10.1002/wcms.30
29. Horonovskyi Y.T., Nazarenko Yu.P., Nekriach E.F. *Kratkyi spravochnyk po khymyy*. Piatoe yzdanye. (Kyev: Naukova Dumka, 1987). [in Russian].

СТІЙКІСТЬ ОДНОАТОМНИХ КОМПЛЕКСІВ ЗАЛІЗА НА ГРАФЕНІ З ПОДВІЙНОЮ ВАКАНСІЄЮ

О.С. Карпенко, В.В. Лобанов, М.Т. Картель

Інститут хімії поверхні імені О.О. Чуйка Національної академії наук України, вул. Генерала Наумова, 17, Київ, 03164, Україна. E-пошта: karpenkooksana@ukr.net

*Методом DFT (B3LYP) у базисі 6-31 G** із залученням поправок Гріме (для врахування дисперсійних взаємодій) розглянуто рівноважну та просторову будову молекули поліциклічного ароматичного вуглеводню $C_{96}H_{24}$, яка обрана як модель графенової площини, а також систем, отриманих з неї видаленням двоатомної молекули C_2 ($C_{94}H_{24}$) з наступною заміною чотирьох атомів Карбону на чотири атоми Нітрогену ($C_{90}N_4H_{24}$). У цьому ж наближенні вивчено енергетику утворення комплексу атома заліза в нульовому ступені окиснення (Fe^0) з $C_{90}N_4H_{24}$ ($[C_{90}N_4H_{24}Fe]^0$) у пласкому квадратному полі ліганда. Визначено типи молекулярних орбіталей ліганда, які за симетрією відповідають симетрії атомних d-орбіталей атома Fe. Побудовано діаграми взаємодії d-орбіталей атома заліза з деякими молекулярними орбіталями ліганда $C_{90}N_4H_{24}$ відповідної симетрії. Зроблено висновок про те, що зв'язування атома перехідного металу на подвійній вакансії графенової площини можливо раціонально описати, виходячи з локальної симетрії координаційного центру і молекулярних орбіталей ліганда та утвореного комплексу.*

Ключові слова: *графен допований залізом, поліциклічний ароматичний вуглеводень, теорія функціоналу густини, дефектовмісний графен, подвійна вакансія, атом перехідного металу, теорія поля лігандів.*